



TRANSPORT IN MESOSCOPIC SEMICONDUCTOR STRUCTURES

A Project submitted to the program of Graduate Programs of Addis Ababa University in Partial Fulfillment of the Requirements

For

The Degree of Masters of Science in Physics

(CONDENSED MATTER)

BY

TSEGAYE FELEKE

March, 2021

Addis Ababa, Ethiopia

ABSTRACT

A review on charge transport in mesoscopic semiconductor structure was presented by considering the quantum transport theory of carrier and quasi particles in low-dimensional structures called semiconductor nanostructure devices. More specifically, the concentration, motions and optical properties of carriers in a semiconductor crystal structure are theoretically as well as statistically described based on Fermi – Dirac distribution and Boltzmann transport equation. We reviewed the free-carrier and free-quasi particle transport in semiconductor nanostructure devices based on the well-known non equilibrium Green function approach. The effects of interference on Aharonov-Bohm limit, the general properties of scattering super operators entering the effective quantum transport theory at various description level reduction procedure and diagonal or semiconductor limit were also reviewed separately.

ACKNOWLEDGEMENTS

First of all I would like to thank God, for giving me the strength and for letting me to accomplish this study. Secondly my deepest and hearts felt gratitude goes to my advisor and instructor Dr. Tesgara Badassa for his invaluable advices, guidance, comment, continuous support and friendly approach throughout this study. I extend my heartfelt gratitude to my family, I owe special thanks to my wife Belyou Silish and my daughters Finot Tsegaye, Yeabsira Tsegaye, Habel Tsegaye for their various support and encouragement during my study. Finally I would like to thank my sponsor, Ministry of Education and AAU for providing the opportunity to suite my MSc and the necessary research funds.

Tsegaye Feleke

March, 2021

Table of Contents

ABSTRACT..... I

ACKNOWLEDGEMENTS II

INTRODUCTION 1

CHAPTER ONE 6

 1. 1 THEORY OF SEMICONDUCTOR..... 6

 1.1.1 *Intrinsic Semiconductors The Concept of a Hole*..... 8

 1.1 .2 *Impurity Semiconductors*..... 10

CHAPTER-TWO 12

 2.1 PHYSICAL SYSTEM 12

 2.2 TRANSPORT IN MESOSCOPIC SEMICONDUCTOR STRUCTURE 13

 2.3 TWO-DIMENSIONAL ELECTRON GAS IN SEMICONDUCTOR HETERO STRUCTURES.... 14

 2.4 EFFECTIVE MASS APPROXIMATION 16

 2.6 BALLISTIC ELECTRON TRANSPORT..... 20

 2.6.1 *Scattering Mechanisms In Hetero Structures*..... 21

 2.7 CONDUCTANCE: LANDAUER-BÜTTIKER APPROACH..... 23

 2.7.1 *Landauer Formula*..... 23

 2.7.2 *Linear Response* 26

CHAPTER-THREE 30

 3.1 TRANSPORTS IN VIBRATIONAL MODES 31

 3.2 CORRELATION AND SCATTERING FUNCTIONS 31

 3.3. NON EQUILIBRIUM TECHNIQUES IN MESOSCOPIC TUNNELING STRUCTURES 33

 3.4. MODEL HAMILTONIAN 33

 3.4.1. *Contact Hamiltonian* 34

 3.4.2. *Tunneling Hamiltonian*..... 34

 3.4.3. *Central Region Hamiltonian* 35

 3.4.3.1. *Central region in non- interacting levels*.....35

 3.4.3.2. *Central region couple to phonon*.....35

 3.4.3.3. *Anderson-type model (electron-electron interactions)*.....35

 3. 5.GENERAL EXPRESSION FOR THE CURRENT 36

 3.6 CURRENT CONSERVATION 37

3.7 NON INTERACTING RESONANT-LEVEL MODEL	39
SUMMARY AND CONCLUSION	42
Bibliography	45

INTRODUCTION

Study of mesoscopic phenomena is one of the most active areas of today's solid state physics. One can observe signatures of mesoscopics in a large number of different physical systems, and it would be impossible in the present context to cover all the possible variations of the mesoscopic theme. We restrict ourselves exclusively to the particular subclass which can be studied in semiconductors. Thus the generic system we have in mind is a semiconductor hetero structure where charge carriers are introduced either by modulation doping, or they flow in and out of the system through heavily doped (metallic) contacts. Transport physics in these systems can roughly be divided into two categories: perpendicular transport and parallel transport, according to whether the charge carriers' motion is perpendicular or parallel to the layers that form the hetero structures. A representative example of perpendicular transport is the resonant-tunneling diode (RTD), which consists of alternate layers of semiconductor materials with different band gaps; a schematic conduction band diagram is shown in Fig. 1. 1 Charge carriers entering from left may, at a certain bias voltage, be tuned to the quasi bound state in the quantum well, which results in a large enhancement of the transmitted current.

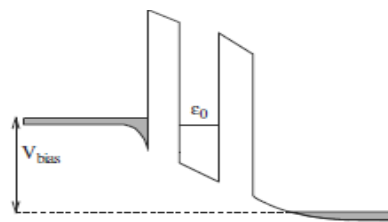


Fig.1.1. Double-barrier semiconductor hetero structure biased close to resonance, where, charge carriers emerging from the source contact are matched to the energy of the quasi bound state ϵ_0 in the quantum well. Occupied contact states are shown as hatched, and the band bending is due to charge accumulation or depletion.

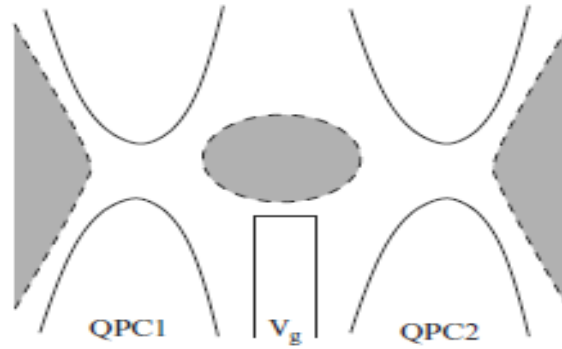


Fig .1.2 Coulomb island, which consists of two tunable quantum point contacts QPC1 and QPC2, and a side gate which allows one to vary the chemical potential, and hence the charge density in the central region. The two-dimensional electron gas underlying the gate structure is depleted outside the hatched regions.

We note that the generic energy-level diagram shown in Fig.1.1 also applies to the emerging field of molecular electronics: there the discrete level(s) in the central region correspond to molecular levels, the “barriers” could be the vacuum gap, and the “doped contacts” could be the metallic electrodes between which the molecule is placed. In the case of parallel transport much attention has been devoted to quantum point contacts (QPC), see Fig. 1.2 for a typical experimental configuration, and other structures based on similar ideas.

Quantum point contacts are based on a split gate geometry: here, at sufficiently high negative gate voltages, the effective connection between the two unmodulated electron gases (“source” and “drain”) is so narrow that perpendicular mode quantization becomes observable, and the measured conductance is an integer multiple of the quantum unit of conductance, e^2/h . The patterns illuminated in an optical photo resist have to be transferred into structured device. Process like developing the photo resist, semiconductor etching, metal evaporation, alloying or selective doping must be carried out without losing the resolution. Furthermore, the devices must be connected to wires, and the inevitable heating generated during operation must be kept under control. Suppose that nano scientists find adequate solutions to all these technological problems –by external electric fields get compensated by many kinds of relaxation processes, which generate frictions. In a

stationary state, these friction forces balance the effects of the external field, and the resistivity of the sample can be defined.

What happens for device sizes comparable to the mean free path, or to other relevant length scales? Well, we then enter the regime of mesoscopic transport. In the following section, we will look at the specific length and energy scales somewhat more closely and give examples for typical transport properties of samples in the mesoscopic regime.

What characterizes the mesoscopic regime? The answer depends on the particular quantity under study. For the above example, the criterion would be that the device size must be comparable to or smaller than the electronic mean free path ℓ_e . Other length scales are the de Broglie wavelength of the electrons that carry the current, which in all cases studied in this book are those electrons at there is in fact little doubt that they will. Then, however, another issue will become more and more important: all the above consideration implicitly assume that the components of a microchip can be scaled down arbitrarily without changes in their performance. This is not the case! Conventional transport theory makes presumptions about certain length and energy scales. For example, it is assumed that the electron mean free path is small compared to the feature size of the device, like the gate length of a transistor. The concept of resistivity is based on this assumption. The hallmark of mesoscopic phenomena is the phase coherence of the charge carriers, which is maintained over a significant part of the transport process. The interference effects resulting from this phase coherence are reflected in a number of experimentally measurable properties. Weak localization can be understood as an increased return probability (and hence increased resistance) due to *coherent* backscattering of charge carriers.

Another example where phase coherence is central is the Aharonov–Bohm effect, where interference of two different transports paths in a ring geometry results in an oscillatory magneto resistance. Yet another example is universal conductance fluctuations, where the conductance of a sample displays rapid changes on the scale of e^2/h (hence the “universality”) when an external control parameter is changed. The external parameter could be magnetic field, or thermal cycling, and the fluctuations reflect changes in the

conducting channels either due to different impurity configurations (thermal cycling), or differences in the way the conduction channels are located in the sample (magnetic field).

It is natural to divide mesoscopic transport into stationary and time dependent phenomena, and we shall take this route by first treating stationary transport and then later turn our attention to time-dependent phenomena. A central issue will be the treatment of interactions in the mesoscopic region, and, as we shall see, non-equilibrium Green function techniques are well suited for this purpose. In the beginning of 1990's a number of authors studied the steady-state situation. The modern reformulation of these ideas, has led to a veritable explosion in the number of papers addressing these issues (there are more than a thousand articles since 1992 which use the Keldysh approach to interacting mesoscopic transport). A key issue is that under certain conditions (to be discussed later) a Landauer-type conductance formula can be derived. The Landauer formula relates the conductance g of a mesoscopic sample [which is connected via "ideal" leads to two (or more) reservoirs] to its transmission properties, $g = (e^2/h) T$, where, T is the quantum mechanical transmission coefficient of the sample. Conductance formulae have played an important role in the analysis of many mesoscopic transport phenomena, and it is therefore of interest to investigate whether interactions and/or time-dependence can be treated in a similar fashion.

The objective of the project is to review the charge transport in mesoscopic semiconductor structures based on the non-equilibrium Green function and Landauer formula. In the first part the idea is to find a way to induce finite transport properties in mesoscopic semiconductors, to achieve this goal, I refer models formed from GaAs/AlGaAs semiconductor heterostructures. The second goal of this project is to show that current is conserved by using non-equilibrium green function approach.

The present project consists of four chapters. Chapter 1 is about the introductory part in which we summarize preliminary concepts of quantum mechanical electronic transport in mesoscopic systems. We focus on the conductivity and concentration of charge carriers in semiconductor materials based on the dependence of temperature. The backbone of this project are chapter 2 and chapter 3, they contain models, applied methods and the results obtained in the study of the quantum transport phenomena of two-dimensional electron gas

(2DEG) and conservation of current by the Landauer-Büttikerformalism and non-equilibrium green function approach. Chapter 4 is about the conclusion and summary.

CHAPTER ONE

LITERATURE PREVIEW

1. 1 Theory of Semiconductor

The band theory enables us to explain why some solids are conductors, some are semiconductors and others are dielectrics. At low temperatures, pure semiconductors behave like insulators. Under higher temperatures or light or with the addition of impurities, however, the conductivity of semiconductors can be increased dramatically, reaching levels that may approach those of metals. The common semiconductors include chemical elements and compounds such as silicon, germanium; selenium, gallium arsenide, zinc selenide, and lead telluride.

The physical properties of semiconductors are studied in solid-state physics and semiconductor devices. In this chapter we study theoretical description of charge carriers and the dependence of their concentration n , on which the conductivity through temperature T and energy gap.

The increase in conductivity with temperature, light, or impurities arises from an increase in the number of conduction electrons, which are the carriers of the electrical current. Although the Fermi surface is relevant mostly to metals, the Fermi level is one of the important parameters in theory of semiconductors.

We can characterize semiconductor by energy gap, E_g , between the top of the highest filled band (s) and the bottom of the lowest empty band(s). A solid with an energy band will be non-conducting at $T = 0$ (unless the DC electric field is so strong and the energy gap is so minute that electric break down (ea $E \ll E_g^2/\epsilon_F$) can occur or unless the AC field is of such high frequency that $\hbar\omega$ exceeds the energy gap).

However, when the temperature is not zero there is a non-vanishing probability that some electrons will be thermally excited across the energy gap into the lowest unoccupied levels in the highest occupied bands, which are called, in this context, the conduction bands, leaving behind unoccupied levels in the highest occupied bands, called valence bands. The

thermally excited electrons are capable of conducting, and the hole-type conduction can occur in the band out of which they have been excited.

Solids that are insulators at $T = 0$, but whose energy gaps are of such a size that thermal excitation can lead to observable conductivity at temperatures below the melting point, are known as semiconductors. The distinction between a semiconductor and insulator is not a sharp one, but roughly speaking the energy gap in most important semiconductors is less than 2 eV and frequently as low as a few tens of electron volt.

Since the number of electrons excited thermally into the conduction band (and therefore the number of holes they leave behind in the valence band) varies exponentially with $1/T$, the electrical conductivity of semiconductors should be very rapidly increasing function of temperature in contrast to the case of metals. The conductivity of metals $\delta = \frac{e^2 n \tau_F}{m}$, declines with increasing temperature, for the density of carrier's n is independent of temperature, and all temperature dependence comes from the relaxation time, which generally decreases with increasing temperature because of increasing in electron-phonon scattering.

The relaxation time in semiconductors will also decrease with increasing temperature, but this effect (typically described by a power law) is quite overwhelmed by the very much more rapid increase in the density of carriers with increasing temperature. This is the most striking feature of semiconductors is that, unlike metals, their electrical resistance declines with rising temperature; i.e., they have a "negative coefficient of resistance."

It was observed that the thermo powers of semiconductors were anomalously large compared with that of metals (by a factor of 100 or so), that semiconductors exhibited the phenomenon of photoconductivity, and that rectifying effects could be obtained at the junction of two unlike semiconductors. Early in the twentieth century, measurements of Hall-effect were made confirming that the temperature dependence of the conductivity was dominated by that of the number of carriers, and indicating that in many substances the sign of the dominant carrier was positive rather than negative.

Within the band theory they find simple explanations. For example, photoconductivity (the increase in conductivity produced by shining light on a material) is a consequence of the fact if the band gap is small, then visible light can excite electrons across the gap into the conduction band, resulting in the conduction by those electrons and by the holes left behind. In a pure, or intrinsic, semiconductor such as silicon, the valence electrons, or outer electrons, of an atom are paired and shared between atoms to make a covalent bond that holds the crystal together. These valence electrons are not free to carry electrical current. To produce conduction electrons, temperature or light is used to excite the valence electrons out of their bonds, leaving them free to conduct current. Electrons are excited from the lower valence band to the upper conduction one. Deficiencies, or holes, are left behind that contribute to the flow of electricity.

This is the physical origin of the increase in the electrical conductivity of semiconductors with temperature. The energy required to excite the electron and holes should be of the order of the energy gap. Thus, at finite temperatures there are holes in the valence band and the electrons in the conduction band.

The modern way to produce materials for electronics is to dope semiconductor material with impurity atoms which introduce carriers in a controllable way.

1.1.1 Intrinsic Semiconductors the Concept of a Hole

Semiconductors containing a negligible amount of electro-active defects (chemical and crystallographic) are termed intrinsic semiconductors. Examples are germanium, silicon, selenium, tellurium, III-V chemical compounds such as indium antimonite (InSb), gallium arsenide (GaAs), and silicon carbide (SiC).

At absolute zero the valence band of intrinsic semiconductors is completely filled and the conduction band, which is at a distance E_g above, is empty. For this reason, at absolute zero intrinsic semiconductor is a dielectric. As temperature increases the electrons of the valence band become excited and some of them receive enough energy, jump the forbidden band and go to the conduction band. This results in free conduction electrons appearing in the conduction band and free electron levels capable of accepting valence band electrons appearing in the valence band. The crystal becomes conductors. The narrower the

forbidden band and the higher the crystal temperature the greater the number of electrons going to the conduction band, and correspondingly, the greater the electrical conductivity of the crystal.

Two important conclusions may be drawn from the discussion.

1) The electrical conductivity of intrinsic semiconductors is an excited: it appears only as the result of the action of external factor capable of imparting sufficient energy to the electrons of the valence band to move them to the conduction band. Such factors may be heating of the semiconductor and irradiation with light or with ionizing radiation.

2) The division of a material into semiconductor and dielectric is essentially a matter of convention. Diamond, a dielectric at room temperature, exhibits a noticeable conductivity at higher temperatures and may also be considered as semiconductor.

As the result of transition of some electrons close to the top of the valence to the conduction band, some free levels appear in the valence band. If an external field is applied to the valence band the electrons, they can go to the free levels and establish electric current. This electric current is given by:

$$J = -q \sum_i V_i \quad (1.1.1)$$

Hence the current due to electrons in the valence band with one vacant state is equivalent to a current set up by the motion of a positive charge q occupying the respective state. Such a fictitious particle is called a hole. If we attribute to the hole a positive charge $+q$ numerically equal to the electron charge, we should also attribute it a positive effective mass m_p^* , numerically equal to the negative effective mass of electron (at that position) m_n^*

$$q_p = -q_n; \quad m_p^* = -m_n^*$$

Only in this case will the current established by holes coincide both in magnitude and direction with the current produced by the electrons of almost filled valence band. Thus, all the parameters of holes are determined by the parameters of the valence band electrons. The hole drift velocity is directed in the direction of the field, $v_p = \mu_p E$, whereas the bound electron velocity is against the field. Note also that in intrinsic semiconductors charge

carriers (electrons and holes) are created or destroyed in pairs and simultaneously so that always the electron concentration n hole concentration p are equal

$$p = n = n_i \quad (1.1.2)$$

where n_i is the intrinsic carrier concentration.

1.1. 2 Impurity Semiconductors

Semiconductors no matter how pure they are always contain some impurity atoms, which create their own energy levels termed impurity levels. These levels may occupy positions both inside the allowed and forbidden bands of the semiconductor at various distances from the top of the valence band and from the bottom of the conduction band. Frequently impurities are introduced intentionally to impart specific properties to the semiconductors. For example the addition of boron to silicon in the proportion of 1boron to 10^5 silicon atoms increases the conductivity of pure silicon by a factor of 10^3 . The deliberate addition of impurities to a semiconductor is called doping. The types of impurity levels situated inside forbidden band are donor and acceptor levels.

The impurities that supply electrons are termed donors and the energy levels of such impurities are donor levels .Semiconductors doped with donor impurities are termed n-type semiconductors.

The impurities that trap electrons from the valence band are termed acceptors and the energy levels of such impurities acceptor levels. The semiconductors doped with such impurities are termed p-type semiconductor. Thus, if the electron concentration is n and the hole concentration is p , the current density is given by;

$$J = (en\mu_e + ep\mu_p) E \quad (1.1.3)$$

The mobility μ is the magnitude of the drift velocity per unit electric field

$$\begin{aligned} \mu &= V/E \quad , \\ \mu_e &= e\tau_e/m_e \quad , \quad \mu_p = e\tau_p/m_p \end{aligned} \quad (1.1.4)$$

Then, the conductivity of semiconductor is given by;

$$\sigma = en\mu_e + ep\mu_p \quad (1.1.5)$$

To solve the tunneling problems in non-equilibrium perturbation scheme one can recognize that how the technique in part II can be used to drive the non-equilibrium perturbation scheme for mesoscopic system. This 2-DEG features an extremely low scattering rate. The mobility μ , defined as the ratio of the drift velocity to the electric field, provides a direct measure of the momentum relaxation time as limited by impurities and defects. Mobility measurement using the Hall-effect is a basic characterization tool for semiconducting films. Electronic conduction in semiconductors takes place either by electrons in the conduction band or holes in the valance band. In mesoscopic system experiments, electron flow usually dominates.

CHAPTER TWO

THEORETICAL BACKGROUND

2.1 Physical system

The core region of typical nanostructure devices like semiconductor super lattices, double barrier structures and quantum dots the overall behavior of such quantum systems is the results of nontrivial interplay between phase coherence and energy relaxation/dephasing. It follows that a proper treatment of such novel nanoscales devices requires a theoretical modeling able to properly account for both coherent and incoherent, i.e., phase-breaking, processes on the same footing with in a many-body picture. By employing non equilibrium Green function formalism for the study of various semiconductor nanostructures as well as of modern micro/optoelectronic devices .To provide a general formulation of quantum charge transport in semiconductor nanostructures, let us consider a generic carrier gas with in a semiconductor crystal in the presence of electromagnetic fields. The corresponding Hamiltonian can be schematically written as

$$\hat{H} = \hat{H}_0 + \hat{H}'$$

The first term,

$\hat{H}_0 = \hat{H}_0^C + \hat{H}_0^{qp} = \sum_{\alpha} \epsilon_{\alpha} \hat{C}_{\alpha}^{\dagger} \hat{C}_{\alpha} + \sum_q \epsilon_q \hat{b}_q^{\dagger} \hat{b}_q$, is the sum of the free-carrier and free-quasiparticle Hamiltonians, where the Fermionic operators $\hat{C}_{\alpha}^{\dagger}(\hat{C}_{\alpha})$ denote creation (destruction) of a carrier in the single-particle state α (with energy ϵ_{α}), while the Bosonic operators $\hat{b}_q^{\dagger}(\hat{b}_q)$ denote creation (destruction) of a generic quasi particle excitation with wave vector q and energy ϵ_q , i.e., phonons, photons, Plasmons, etc.

The second term, \hat{H}' , is the sum of all possible carrier-carrier as well as carrier-quasiparticle interaction Hamiltonians, i.e., carrier-phonon, carrier-photon, carrier-Plasmon, etc. The non interacting carrier-plus-quasi particle basis states are given by Eigen states of \hat{H}_0 : the generic Eigen state $|\lambda\rangle = |\{n_{\alpha}\}\rangle \otimes |\{n_q\}\rangle$ is the tensor product of non interacting carrier and quasi particle states corresponding, respectively, to the occupation numbers $\{n_{\alpha}\}$ and $\{n_q\}$, while the non-interacting energy spectrum

$\epsilon_\lambda = \sum_\alpha \epsilon_\alpha n_\alpha + \sum_q \epsilon_q n_q$ is the sum of the total carrier and quasi particle energies.

Most of the electronic properties of interest in the analysis of charge transport phenomena in semiconductor nanostructures are single-particle quantities, i.e., physical quantities ascribed to the generic particle in our electronic subsystem, like carrier drift velocity, mean kinetic energy, etc.

2.2 Transport in Mesoscopic Semiconductor Structure

During the 1980s, an important question arose, namely, what new effects emerge when the dimension of a small conductor is between microscopic and macroscopic sizes? One of these effects is the quantization of conductance meaning that Ohm's law does not hold for sufficiently small conductors.

An example of conductance quantization that is related to quantum point contacts

(QPCs) is shown in Fig. 2.1 In this experiment, the conductance of the QPC is measured as a function of its (negative) gate voltage. Referring to the behavior shown in the inset, as the gate voltage gets below $\sim -0.5V$, a sudden drop in the conductance is observed, indicating the full depletion of the 2-DEG directly underneath the gates and, thus, the formation of the QPC. As this gate voltage is made even more negative, a slower decrease of the conductance occurs and it is clear from the behavior in the main panel that it develops into a step like behavior. In fact, the conductance in this figure is plotted in units of $2e^2/h$ and it is clear that each step in the conductance corresponds to a change by this amount. The h/e^2 is referred to as the von Klitzing constant [3]. This remarkable behavior was first observed, independently, by Wharam et al. [4] and van Wees et al. [5] and has been confirmed in numerous experiments [6].

The purpose of the current chapter is to recall the fundamental ideas and properties of semiconductor nanostructures and quantum transport effects.

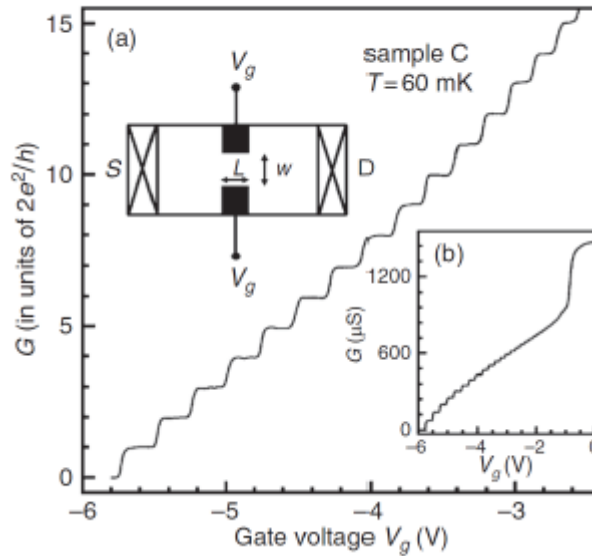


Fig.2.1 The conductance G of a QPC measured as function of the gate voltage V_g at low temperature. The quantum mechanical phenomena are expressed by the step like behavior of G .

2.3 Two-Dimensional Electron Gas in Semiconductor Hetero Structures

In this section we summarize some basic concepts related to two-dimensional electron gas systems. As an example, we discuss the gallium arsenide (GaAs) / aluminum gallium arsenide (AlGaAs) material system which provides a very high quality two-dimensional transport channel and has been widely used in artificial nanostructures [2]. These systems opened a new research area, namely, the physics of the electronic properties of two dimensional structures. In order to understand the importance of semiconductor hetero structures in mesoscopic systems, let us take a look at the band scheme of an AlGaAs and GaAs hetero junction shown in Fig. 2.2. As it is known, the n-type AlGaAs can be doped with donor impurities. As we can see, the Fermi energy E_f in the wide gap AlGaAs layer is higher than in the narrow gap GaAs layer. Consequently electrons move away from the n-AlGaAs part of the sample leaving positively charged donors behind. Because of the positive excess charge, an electrostatic potential arises that causes the bands to bend as shown in Fig. 2.2. At equilibrium and in the absence of bias, the Fermi energy becomes constant in the whole semiconductor structure. However, the electron density is sharply peaked close to the GaAs–AlGaAs interface (where the Fermi energy is inside the

conduction band). It is forming a thin conducting layer which is usually referred to as a two-dimensional electron gas (2-DEG).

The carrier mobility of semiconductor hetero structures can be considerably larger than that of the corresponding bulk semiconductor; this is achieved by a technique generally referred to as "modulation doping". Modulation-doped hetero structures are obtained by introducing n-type dopant impurities into the wide-band-gap AlGaAs at some distance from the interface (the undoped AlGaAs is called the spacer), whereas the narrow-band-gap material (GaAs) remains free from intentional doping, as shown in Fig. 2.2(a). Due to modulation doping [10], the mobile carriers in the hetero structure are spatially separated from their parent impurities [12], which lead to a reduction of scattering. Thus, high carrier mobility can be obtained [8]. The charge carrier concentration in a 2-DEG generally ranges from $2 \times 10^{11} \text{ cm}^{-2}$ to $2 \times 10^{12} \text{ cm}^{-2}$ and can be depleted by applying a negative voltage on a metallic gate deposited on the surface. The importance of this structure lies in its use as a field effect transistor (FET).

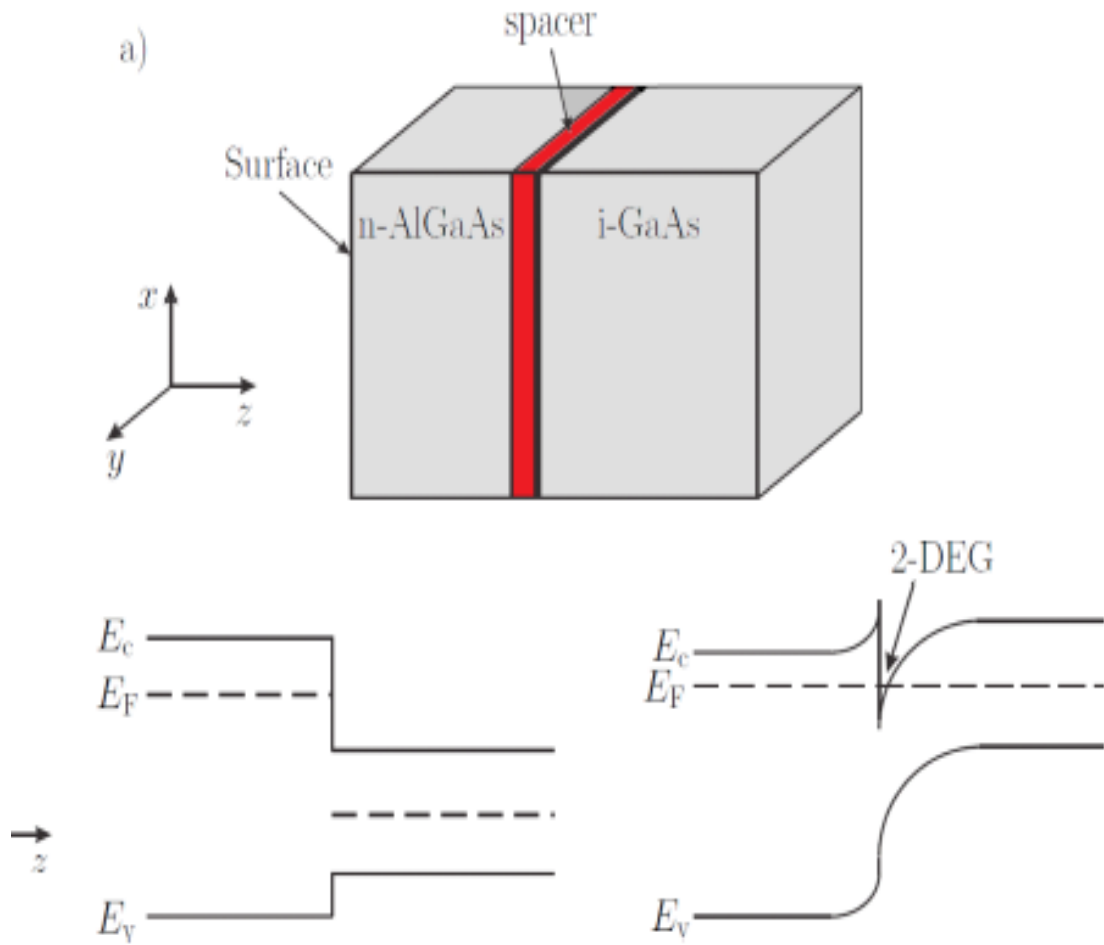


Fig. 2.2: Conduction and valence band line-up at a junction between an n-type AlGaAs and intrinsic GaAs, (a) before and (b) after charge transfer has taken place. Note that this is a cross-sectional view [8, 9].

2.4 Effective Mass Approximation

The dispersion relation of Bloch electrons can be approximated by the quadratic expression of wave number vectors k close to the minima of the bands. In a crystal which has a cubic unit cell, if the minimum is located at k_0 , due to the high symmetry, we can write

$$\varepsilon k \approx \varepsilon k_0 + A(k - k_0)^2, \quad (2.4.1)$$

where, ε_k denotes the k -dependent energy and the coefficient $A = \frac{\hbar^2}{2m^*}$.

As interpretation, one can argue that in the dispersion relation of the Bloch electrons, instead of ordinary electron mass m_e , a modified "mass" m^* has appeared. m^* is called the *effective mass* [11], and it is given by

$$\frac{1}{m^*} = \frac{1}{\hbar^2} \frac{\partial^2 \varepsilon_k}{\partial k^2} \quad (2.4.2)$$

The effective mass depends on the periodic potential of the crystal lattice.

In a more general case, the effective mass tensor should be introduced instead of the scalar effective mass (2.4.2):

$$\left(\frac{1}{m^*} \right)_{i,j} = \frac{1}{\hbar^2} \frac{\partial^2 \varepsilon_k}{\partial k_i \partial k_j}, \quad i, j = x, y, z \quad (2.4.3)$$

Now we can write the electron energy in the following form

$$\varepsilon_k \approx \varepsilon_{k0} + \frac{\hbar^2}{2} \sum_{i,j} \left(\frac{1}{m^*} \right)_{i,j} (k_i - k_{oi})(k_j - k_{oj}) \quad (2.4.4)$$

As it is known, there are several methods which can be used for the derivation of the effective-mass approximation. One of the possible ways is to use Wannier functions [12, 13]. However, considering our aims, a Schrödinger-like equation is more suitable.

Within the framework of the effective mass approximation, the dynamics of the electrons in the conduction band is governed by the following equation:

$$H_{eff} \Psi(r) = \left[E_c + \frac{1}{2m^*} (i \hbar \nabla + eA)^2 + U(r) \right] \Psi(r) = E \Psi(r). \quad (2.4.5)$$

Where the conduction band edge is denoted by E_c and the potential term $U(r)$ appears owing to space-charges and confinement. When an external electromagnetic field interacts with the electronic system, one uses the transformation $i \hbar \nabla \rightarrow i \hbar \nabla + eA$. It is called minimal or Peierls substitution [14] that has several different aspects in the theory of Bloch electrons as well as in more general quantum mechanical problems [15, 16].

Let us emphasize, that the effective mass m^* is distinct in different bands. Thus the relation (2.4.5) is valid inside a given band. The lattice potential does not appear explicitly in the effective Hamiltonian H_{eff} , its effect is manifested in the effective mass m^* which we will

assume to be spatially independent. Any band discontinuity ∇E_c at the hetero junction is incorporated by letting E_c be position-dependent. According to these, Eq. (2.4.5) is usually referred to as the single-band effective mass equation.

2.5 Transverse modes and sub band structure

Our aim is to understand the quantum mechanical behavior of electrons which are confined in a narrow channel. To this end, we consider a simple model of an ideal quantum channel with transverse modes. Such a rectangular conductor is shown schematically in Fig. 2.3 (a). We assume the horizontal length of the wire in x-direction to be very long compared to its cross-sectional area. The motion of charge carriers (in the present case, electrons) in a narrow quantum channel is described by the effective mass equation;

$$[E_c + \frac{1}{2m^*} (i\hbar\nabla + eA)^2 + U(y)]\psi(x, y) = E\psi(x, y) \quad (2.5.1)$$

The solutions to Eq. (2.5.1) can be expressed in the form of plane waves (L: length of conductor over which the wave function is normalized)

$$\Psi(x, y) = \frac{1}{\sqrt{L}} \exp[ikx] \chi(y). \quad (2.5.2)$$

where the function $\chi(y)$ describes the transverse mode.

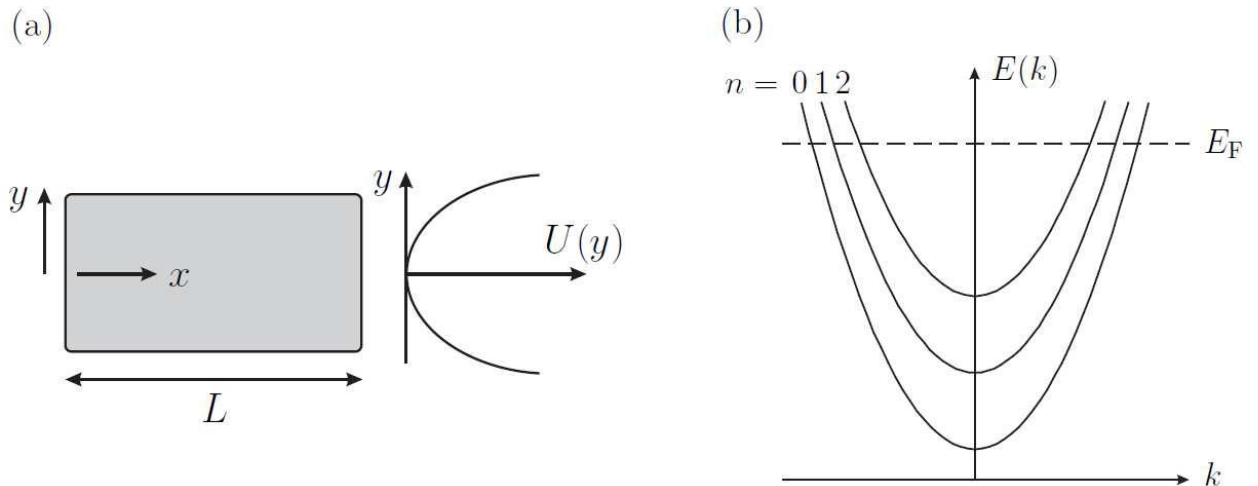


Fig. 2.3: Panel (a) shows a rectangular conductor assumed to be uniform in the x direction.

It has a transverse confining potential $U(y)$. Panel (b): Dispersion relation, $E(k)$ for electric sub bands arising from parabolic confinement. The different sub bands are indexed by n [8].

However, we can find an adequate description of various physical problems [17, 18] if $U(y)$ can be approximated by a quadratic potential

$$U(y) = \frac{1}{2} m \omega_0^2 y^2 \quad (2.5.3)$$

In this case, the mode functions $\chi_{n, k}(y)$ and the corresponding Eigen energies $E(n, k)$ can be obtained using the theory of the quantum linear harmonic oscillator [19]. They are given by:

$$\chi_{n, k}(y) = U_n(q) \text{ where } q = y \sqrt{\frac{m \omega_0}{\hbar}}, \quad (2.5.4)$$

$$E(n, k) = E_c + \frac{\hbar^2 k^2}{2m} (n + \frac{1}{2}) \hbar \omega_0, n = 0, 1, 2, \dots, \quad (2.5.5)$$

where,

$$U_n(q) = \exp\left[\frac{-q^2}{2}\right] H_n(q) \quad (2.5.6)$$

With $H_n(q)$ being the n^{th} Hermit polynomial [20], and different values of the integer n label the different sub bands.

The most remarkable consequence of the sub band structure is the lifting of the band edge energy by $\varepsilon_n = (n + 1/2) \hbar \omega_0$. This effect is general, appears for any confining potential, although the values of ε_n obviously depend on the choice of $U(y)$. In the following we consider quasi one-dimensional samples, where no other transversal modes are assumed to be excited than the ground state ($n = 0$). This leads to a modification of the effective mass equation:

$$\left[E_s + \frac{1}{2m^*} (i\hbar \nabla + eA)^2 + U(x, y) \right] \Psi(x, y) = E \Psi(x, y), \quad (2.5.7)$$

where $E_s = E_c + \varepsilon_0$. This simplification is applied throughout the project when discussing semiconductor nanostructures.

2.6 Ballistic Electron Transport

There are essentially two qualitatively different regimes of transport: diffusive (ohmic) and ballistic. We can determine which regime is relevant for a given sample by using certain characteristic lengths: the linear size of the sample, the mean free path, and the phase-relaxation length.

We consider a realistic condensed matter model which can include impurity effects, lattice vibrations (phonons) or additional 'collision' mechanisms that scatter the electron from one state to another thereby changing their moment a. The momentum relaxation time τ_m is related to the collision time τ_c by a relation of the form

$$\frac{1}{\tau_M} \propto \alpha_M \frac{1}{\tau_c} \quad (2.6.1)$$

Where, the dimensionless coefficient α_m (it's possible values are in the interval [0,1] denotes the 'effectiveness' of an individual collision in destroying momentum. Accordingly, we can provide the definition of the mean free path Lm : it is the distance that an electron travels before its initial momentum is destroyed. That is,

$$Lm = V_F \cdot \tau_m, \quad (2.6.2)$$

where $V_F = \hbar k_F/m$ is the Fermi velocity. Lm is usually referred to as the momentum relaxation length.

Analogously, we can define the phase-relaxation time (τ_φ) and length ($L\varphi$) by

$$\frac{1}{\tau_\varphi} \propto \alpha_\varphi \frac{1}{\tau_c} \quad (2.6.3)$$

where, the factor α_φ denotes the effectiveness of an individual collision in destroying the phase. One way to visualize the destruction of phase is in terms of a thought experiment involving interference [2]. Let us consider a device which can split a beam of electrons into two paths and then recombine them. Actually, it is an interferometer. In a perfect crystal the two arms would be identical resulting in constructive interference. By applying a magnetic field perpendicular to the plane containing the paths, one can change their relative phase thereby changing the interference from constructive to destructive (and vice versa). Now we take into account a real crystal in which some kind of scattering effects can arise

due to impurities, defects, phonons etc. We would expect the interference amplitude to be reduced by a factor $\exp\left[-\frac{\tau_t}{\tau_\phi}\right]$, where, τ_t is the transit time that the electron spends in the interferometer.

Now we can provide the relation between the phase-relaxation time (τ_ϕ) and the phase relaxation Length (L_ϕ). It can be written as;

$$L_\phi = V_F \tau_\phi \quad (2.6.4)$$

This is valid if the phase-relaxation time is of the same order or shorter than the momentum relaxation time, that is, if $\tau_\phi \sim \tau_m$, which is often the case in a high-mobility semiconductors.

Having recalled basic concepts, the two distinct regimes of transport can be distinguished in an intuitive way: If the length L of the sample is much larger than the phase relaxation length L_ϕ then quantum interference phenomena disappear. That is, when $L_\phi, L_m \ll L$, the description of transport should be based on classical models. This is the *ohmic regime*. On the other hand, when $L_\phi, L_m > L$, the transport properties are determined by quantum interference effects. This is the *ballistic regime*.

2.6.1 Scattering Mechanisms in Hetero Structures

In this section we provide a short overview of the most relevant scattering mechanisms (without claim of completeness) that are present in semiconductor hetero structure samples. We focus on two-dimensional electron gases in which the following scattering mechanisms arise:

- optical phonon scattering (dominant at high temperatures)
- acoustic phonon scattering (deformation potential and piezoelectric effects)
- magnetic impurity scattering
- ionized donor scattering (remote impurity)
- scattering from neutral defects or impurities.

As a reference, Fig.(2.4) shows the influence of different scattering mechanisms the temperature dependent mobility of a bulk GaAs, sample. The role of the scattering mechanisms which are relevant in an optimized 2-DEG in a Ga[Al]As hetero junction be seen in Fig. (2.5).

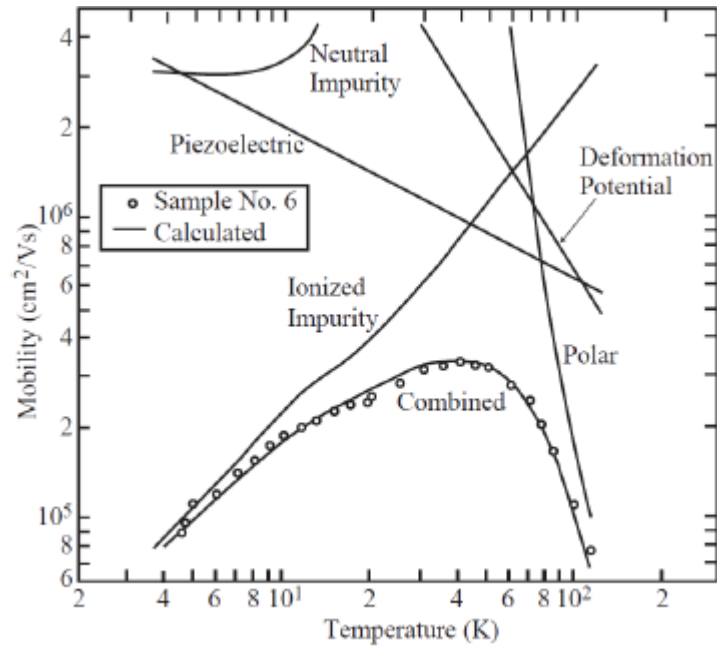


Fig. 2.4: Influence of various scattering phenomena on the temperature dependence of the mobility of a three-dimensional GaAs sample [21].

As we can see in Figure 2.5, scattering effects can strongly limit the mobility of electrons in a 2-DEG. This fact may lead to the disappearance of ballistic electron transport, thus taking them into account is inevitable in realistic calculations.

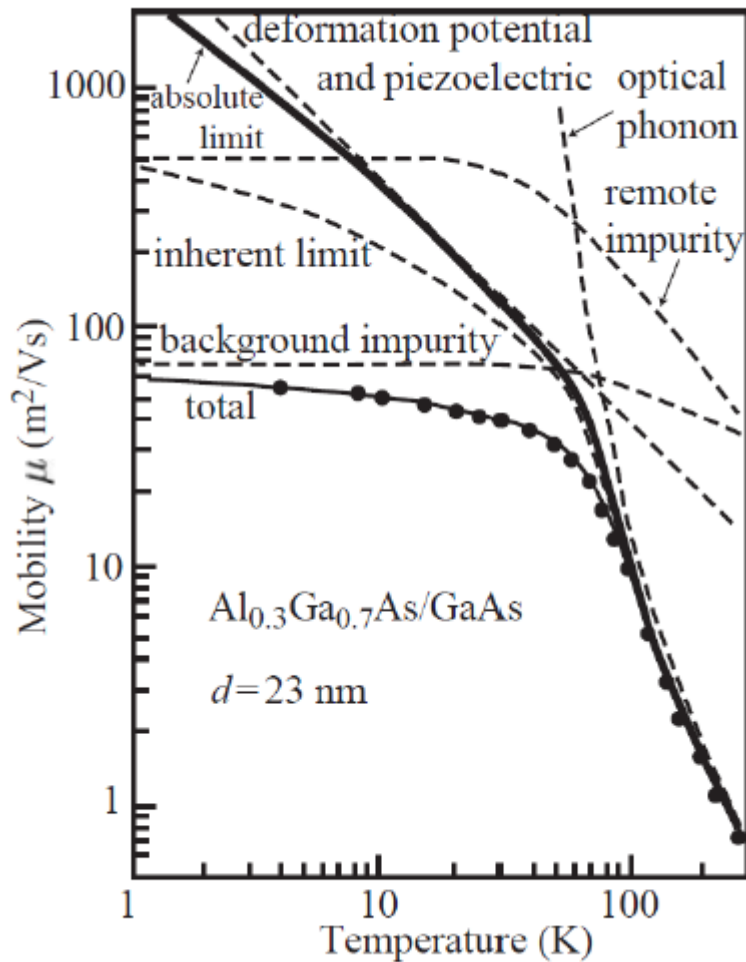


Fig.2.5 Influence of different mechanisms on the mobility of GaAs/AlGaAs hetro structure. The spacer layer thickness is denoted by d [10].

2.7 Conductance: Landauer-Büttiker Approach

2.7.1 Landauer Formula

Let us consider a ballistic conductor which is connected to two electron reservoirs

("Contact 1" and "Contact 2"). They are characterized by the electrochemical potentials μ_1 and μ_2 (see Fig. 2.6 (a)). When the dimensions of the nano devices is large enough, the conductance can be written as $G = \sigma W/L$. Here, the length and the width are denoted by L

and W , and the conductivity σ is a material constant which does not depend on the size of the sample. Let us investigate the behavior of G when $L \rightarrow 0$. Naively, one could expect the conductance to increase indefinitely. However, on the basis of experimental observations, G approaches a limiting value G_C when $L \leq L_m$, i.e., the conductor is much shorter than the mean free path. Our goal is to determine the *contact resistance* G^{-1}_C by calculating the current flowing through a ballistic sample for given *bias* $\mu_1 - \mu_2$. We assume that the contacts are *reflection less*. That is, the electrons can enter the contacts from the sample without reflections. In this case right propagating ($+k$) states in the conductor are occupied only by electrons originating from the left contact while $-k$ states are occupied only by electrons that originate from the right contact. (This holds because charge carriers that enter from the right contact populate the $-k$ states and empty without reflection into the left contact. while the ones that enter from the left contact populate the $+k$ states and empty without reflection into the right contact.) Note that the wave number component in the x direction is denoted by k .

We argue that the quasi-Fermi level F_+ for the $+k$ states is always equal to μ_1 even when a bias $\mu_1 - \mu_2$ is applied (see Fig. 2.6 (b)). If we generate an electrochemical potential difference between left and right contacts, it can have no effect on the quasi-Fermi level F_+ for the $+k$ states since there is no causal relationship between the right contact and the $+k$ states. No electron originating in the right contact ever makes its way a $+k$ states. Similarly quasi-Fermi level F_- for the $-k$ states in the right lead is always equal to μ_2 . Hence at low temperatures the current is equal to that carried by all the $+k$ states lying between μ_1 and μ_2 [2].

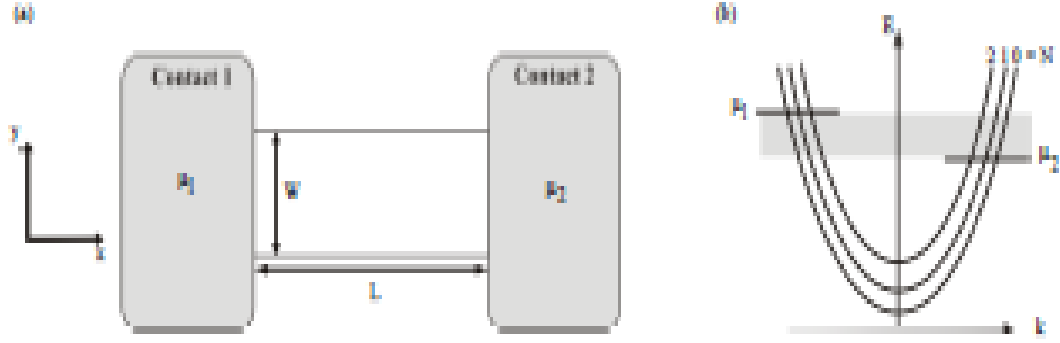


Fig. 2.6: (a) Quantum wire connected to left and right electron reservoirs (gray). The electrochemical potentials of the reservoirs are μ_1 and μ_2 . (b) Dispersion relation in the quantum channel. The gray-shaded energy interval is determined by the applied voltage between left and right reservoirs (bias window) [2].

Before we calculate the current there is an important statement corresponding to different transverse modes, see Fig. 2.6. The dispersion relation $E(N, kx)$ related to the sub band N (Fig. 2.6 (b)) has cut- off energy

$$\varepsilon_N = E(N, kx = 0) \quad (2.7.1)$$

below which no waves can propagate. The number of sub bands that play a role in the conductance at an energy E is obtained by counting the number of modes having cut-off energies smaller than E :

$$M(E) = \sum_N \theta(E - \varepsilon_N) \quad (2.7.2)$$

We can evaluate the current carried by each transverse mode (labeled by subscript N in Fig. 2.6 b) separately and add them up.

First, we take into account a single transverse mode whose $+k$ states are occupied according to the function $f^+(E)$. Let us recognize that if a uniform electron gas with n electrons per unit length move with a velocity of v , it carries a current is equal to env . The electron density is associated with a single k -state in a conductor of length L is given by $1/L$. The corresponding current I^+ can be written as

$$I^+ = \frac{e}{L} \sum V f^+(E) = \frac{e}{L} \sum_K \frac{1}{\hbar} \frac{\partial E}{\partial K} f^+(E). \quad (2.7.3)$$

Assuming periodic boundary conditions and converting the sum over k into an integral according to the usual prescription: $\sum_K \rightarrow 2(\text{for spin}) \times \frac{L}{2\pi} \int dk$

we find

$$I^+ = \frac{2e}{\hbar} \int_{\varepsilon}^{\infty} f^+(E) dE, \quad (2.7.4)$$

where ε is the cut-off energy of the waveguide mode. If we consider a multi-mode channel, the formula for the current I^+ reads

$$I^+ = \frac{2e}{\hbar} \int_{-\infty}^{\infty} f^+(E) M(E) dE \quad (2.7.5)$$

where the function $M(E)$ provides us the number of modes that are below the cut-off energy E . Then, we assume that the number of modes M is constant over the energy range $\mu_1 > E > \mu_2$, and at low temperature we find that

$$I^+ = \frac{2e}{\hbar} M \left(\frac{\mu_1 - \mu_2}{e} \right). \quad (2.7.6)$$

Where, $(\mu_1 - \mu_2)/e$ is the bias voltage. Thus the contact resistance is given by

$G_c^{-1} = \hbar/2e^2 M$. This is the resistance of a ballistic conductor.

As a generalization, the Landauer formula reads [1, 2]:

$$G = \frac{2e^2}{\hbar} MT \quad (2.7.7)$$

Where the average transmission probability is denoted by T and M is the number of modes. Obviously, when the transmission probability equals unity, we recover the case discussed earlier.

2.7.2 Linear Response

The way we recalled the derivation of the Landauer formula in the previous subsection relied on several assumptions. We used a simplified picture which is valid at zero temperature and transport occurred only from the left contact to the right one. We also assumed that the current was carried by a narrow energy channel around the Fermi-level.

This allowed us to write the current as

$$I = \frac{2e}{\hbar} \bar{T}(\mu_1 - \mu_2), \quad (2.7.8)$$

where, \bar{T} denotes the product of the number of modes M and the transmission probability per mode T at the Fermi energy (assumed to be constant over the range $\mu_1 > E > \mu_2$).

Now we consider a more general case where transport takes place in the energy range

$$\mu_1 + nK_B T > E > \mu_2 - nK_B T \quad (2.7.9)$$

Where, n is a small integer and k_B is the Boltzmann constant. Each energy value may correspond to a different transmission T . At this point we include injection from both contacts. The influx of electrons per unit energy from lead 1 is given by

$$i_1^+(E) = \frac{2e}{\hbar} M f_1(E) \quad (2.7.10)$$

while, the influx from lead 2 is given by

$$i_2^-(E) = \frac{2e}{\hbar} M' f_2(E) \quad (2.7.11)$$

Where the number of modes in lead 2 is denoted by M' and $f_1(E)$ ($f_2(E)$) is the energy distribution in lead 1 (lead 2) at non-zero temperatures. The out flux from lead 2 can be written as

$$i_2^+(E) = T i_1^+(E) + (1 - T') i_2^-(E) \quad (2.7.12)$$

While, the out flux from lead 1 is written as

$$i_1^-(E) = (1 - T) i_1^+(E) + T' i_2^-(E) \quad (2.7.13)$$

The current $i(E)$ flowing through the nanostructure is given by

$$\begin{aligned} i(E) &= i_1^+ - i_1^- = i_2^+ - i_2^- \\ &= T i_1^+ - T' i_2^- = \frac{2e}{\hbar} [M(E)T(E)f_1(E) - M'(E)T'(E)f_2(E)] \end{aligned} \quad (2.7.14)$$

If we define the transmission function as $\bar{T} = M(E)T(E)$, Eq.(2.7.14) can be reformulated as

$$i(E) = \frac{2e}{\hbar} [\bar{T}(E)f_1(E) - \bar{T}'(E)f_2(E)] \quad (2.7.15)$$

Assume that $\bar{T}(E) = \bar{T}'(E)$, the total current is given by:

$$I(E) = \int i(E)dE = \frac{2e}{\hbar} \int \bar{T}(E)[f_1(E) - f_2(E)]dE \quad (2.7.16)$$

Why should the transmission function from 1 to 2 be equal to that from 2 to 1 ($\bar{T}(E) = \bar{T}'(E)$)? One could argue that they ought to be equal in order to ensure that there is no current at equilibrium ($i(E) = 0$ when $f_1(E) = f_2(E)$). Nevertheless, this argument only proves that $\bar{T}(E)$ should equal $\bar{T}'(E)$ at equilibrium. When the investigated system is far from equilibrium, the applied bias could change the two transmission functions and could lead to $\bar{T}(E) \neq \bar{T}'(E)$. However, if we assume that there is no inelastic scattering (from one energy to another) inside the device, then it can be shown that $\bar{T}(E)$ is always equal to $\bar{T}'(E)$ for a two-terminal device even in the presence of a magnetic field. [2]

When both contacts of the investigated nano device are held at the same potential, $\mu_1 = \mu_2$, according to Eq. (2.7.16), $f_1(E) = f_2(E) \rightarrow I = 0$. If the state is shifted slightly from equilibrium, the current is proportional to the applied bias. The current from Eq. (2.7.16) can be written as

$$\delta I = \frac{2e}{\hbar} \int ([\bar{T}(E)eq \delta[f_1 - f_2] + [f_1 - f_2]eq \delta[\bar{T}(E)]]dE \quad (2.7.17)$$

Naturally, we recognize that the second term vanishes. We can provide an expansion of the first term as

$$\delta[f_1 - f_2] \approx [\mu_1 - \mu_2] \left(\frac{\partial f}{\partial \mu} \right) eq = \left(\frac{\partial f_0}{\partial \mu} \right) [\mu_1 - \mu_2], \quad (2.7.18)$$

Where, $f_0(E)$ is the equilibrium Fermi function which is given by

$$f_0(E) = \left[\frac{1}{1 + \exp[(E - \mu)/KBT]} \right] \mu - E f \quad (2.7.19)$$

At non-zero temperature, the linear response formula is written as follows

$$G = \frac{e \cdot \delta I}{(\mu_1 - \mu_2)} = \frac{2e^2}{\hbar} \int \bar{T}(E) \left(-\frac{\partial f}{\partial E} \right) dE \quad (2.7.20)$$

In the low temperature limit we can write

$$f_0(E) \approx \theta(E_f - E) \rightarrow -\partial f_0 / \partial E \approx \delta(E_f - E). \quad (2.7.21)$$

Then we reach the expression for the conductance within linear response at zero temperature:

$$G = \frac{2e^2}{\hbar} \bar{T}(E_f). \quad (2.7.22)$$

Each quantity is evaluated in equilibrium and thus linear response refers to an equilibrium property of the system.

CHAPTER-THREE

BASIC QUANTUM KINETIC QUESTIONS

The basic quantum kinetic equation which describes the time evolution of the particle propagator (or, the lesser Green function) $G^<$ is discussed in the formulations due to Kadanoff-Baym and due to Keldysh.

The task of this chapter is to introduce the equations-of-motion (in real time) for the non-equilibrium Green functions (NEGF). These equations will form the basis of all subsequent developments. There are two different, but equivalent, formulations: The Kadanoff–Baym method, and the Keldysh method,

We have chosen not to retrace the original derivations but rather use the analytic continuation rules; this approach allows a concise and systematic derivation.

The contour-ordered Green function has the same Dyson equation as the equilibrium function:

$$G(1,1') = G_0(1,1') + \int d^3x_2 \int d\tau_2 G_0(1,2) U(2) G(2,1') + \int d^3x_2 \int d^3x_3 \int d\tau_2 \int d\tau_3 G_0(1,2) \Sigma(2,3) G(3,1'),$$

where we assume that the non-equilibrium term in the Hamiltonian can be represented by a one-body external potential U . The interactions are contained in the (irreducible) self-energy $\Sigma[U]: \Sigma = 1/2(\Sigma^r + \Sigma^a)$ and $G = 1/2(G^r + G^a)$, and the curly brackets indicates an anti commutator. In equilibrium theory we have encountered the spectral function $a = -2\text{Im}g^r = i(g^r - g^a)$ and the imaginary part of the self- energy, $\gamma = -2\text{Im}\delta^r = i(\delta^r - \delta^a)$, These objects can be generalized to non-equilibrium theory;

$A \equiv i(G^r - G^a)$, and $\Gamma \equiv (\Sigma^r - \Sigma^a)$, using this notations we get:

$$\begin{aligned} [G_0^{-1} - U, G^<] - [\Sigma, G^<] - [\Sigma^<, G] &= 1/2i\{\Gamma, G^<\} - 1/2i\{A, \Sigma^<\} \\ &= 1/2\{\Sigma^>, G^<\} - 1/2\{G^>, \Sigma^<\}. \end{aligned} \quad (3.1)$$

In the second line we used the relation $G^r - G^a = G^> - G^<$, and an analogous relation for the self- energy. Eq. (3.1) is the (generalized) Kadanoff-Baym equation (GKB), and it will form the basis of much of our subsequent discussion.

3.1 Transports in Vibrational Modes

The issue of vibrational effects in molecular electronics has recently drawn a lot of interest because inelastic scattering and energy dissipation inside atomic-scale conductors are of importance for device characteristics, working conditions, and their stabilities. Inelastic effects are important, not only because of their potentially detrimental influence on device functioning, but also because they can open up new possibilities and operating modes. Vibrational effects are often visible in the measured conductance of nanoscopic objects; here we focus on recent experimental studies on free standing atomic

goldwires[22]. Agraït and co-workers used a cryogenic STM tip to first create an atomic-scale gold wire, and then measured its conductance as a function of the displacement of tip, and the applied voltage. The calculational method consists of three steps.

1. The mechanical normal modes and frequencies of the gold chain are evaluated.
2. The electronic structure and electron-vibration coupling elements are evaluated in a

Localized atomic-orbital basis set.

3. The inelastic transport is evaluated using non equilibrium Green functions, with a self-consistent Born approximation self-energy in the Dyson and Keldysh equations for the respective Green functions. The electrical current I_L and the power transfer P_L are then evaluated as:

$$I_L = \frac{e}{h} \int d\epsilon t_L(\epsilon), \quad P_L = \int \frac{d\epsilon}{2\pi\hbar} \epsilon t_L(\epsilon),$$

$$\text{where } t_L(\epsilon) = \text{Tr} \{ \Sigma_L^<(\epsilon) G^>(\epsilon) - \Sigma_L^>(\epsilon) G^<(\epsilon) \},$$

3.2 Correlation and Scattering Functions

In a semi classical picture, it is enough to describe a multiple-electron system by distribution function $f(k)$, which specifies the number of electrons occupying a particular state k . However, in **phase-coherent** conductors electron correlation has to be considered, since the phase-relaxation length is not very short. Phase correlation is nothing but the correlation between electrons with different states. In this case, density *matrix*

$p(k, k') = \psi_k \psi_{k'}^*$ (rather than $f(k)$!) is appropriate to describe the system, which includes additional information regarding phase-corrections.

In general, a two-time-dependent correlation function of the form $G^n(k, k'; t, t')$ (**correlation function** G^n or $-iG^<$) is needed to describe the correlation between the amplitude in state k at time t and that in state k' at time t' . Density matrix $p(k, k'; t)$ is a 'subset' of the correlation function obtained by setting $t' = t$.

$$p(k, k'; t) = [G^n(k, k'; t, t')]_{t'=t} \quad (3.2.1)$$

In a steady-state $\psi(t) = \psi_0 e^{-i\omega t}$ and by using Fourier transformation we can get the energy-resolved information $G^n(k, k'; E)$. This is convenient to describe scattering processes which transfer electrons from one energy to another. If we are only interested in steady-state transport, $G^n(k, k'; E)$ is enough to describe correlation and we don't need $G^n(k, k'; t, t')$. The occupation $f(k)$ function can be written in terms of the correlation function.)

$$f(k) = \int \frac{1}{2\pi} G^n(k, k'; E) dE \quad (3.2.2) \text{ This}$$

is true in any representation. For example in real space the electron density is

$$n(r) = 2 \times \int \frac{1}{2\pi} G^n(r, r, E) dE \quad (3.2.3)$$

where a factor of 2 assumes degeneracy of the two spin components.

G^n refers to the correlation of electrons, while G^p (or $+iG^>$) refers to that of **holes**. The inflow of electrons can alternatively be viewed as outflow of holes, whose number is given by $(1-f)$

In the semi-classical picture the scattering function $S^{out}(k, t)$ tells us the rate at which electrons are scattered out of a state k assuming it is initially full. Like correlation function, in the quantum mechanical picture we need to generalize this concept to include phase-correlation $S^{out}(k, t) \rightarrow \Sigma^{out}(k, k'; t, t')$. Again, in steady-state $\Sigma^{out}(k, k'; E)$ is enough to describe the **out scattering**. Similarly, Σ^{in} describes the **in scattering**. The set of four functions G^n , G^p , Σ^{in} and Σ^{out} provides us with the language needed to include phase correlations into a transport problem. In standard literature the counterpart is $-iG^<$, $+I$

$G^>$, $-i \Sigma^<$ and $+i \Sigma^>$, respectively. The classical analog is f , $(1-f)$, S^{in} and S^{out} , respectively.

3.3. Non Equilibrium Techniques In Mesoscopic Tunneling Structures

We recall that the basic difference between the two approaches is that in non-equilibrium one cannot assume that the system returns to its ground state (or a thermodynamic equilibrium state at finite temperatures) as $t \rightarrow +\infty$. Irreversible effects break the symmetry between $t = -\infty$ and $t = +\infty$, and this symmetry exploited in the derivation of the equilibrium perturbation expansion. In non equilibrium situations one overcomes this problem by allowing the system to evolve from $-\infty$ to the moment of interest (t_0), and then the time evolution from $t = t_0$ back to $t = -\infty$.

The advantage of this procedure is that all expectation values are defined with respect to a well-defined state, i.e. the state in which the system was prepared in the remote past. That one can must treat the two time branches on an equal footing. In the remote past the contact (i.e., the left and right lead) and the central region are decoupled, and each region is in thermal equilibrium.

The equilibrium distribution functions for the three regions are characterized by their respective chemical potentials. The couplings between the different regions are then established and treated as perturbations via the standard techniques of perturbation theory, albeit on the two-branch time contour. It is important to notice that the couplings do not have to be small, e.g., with respect level to spacing or $k_B T$, and typically must be treated to all orders. In certain special cases it has been shown that the two approaches lead to the same asymptotic steady-state current, while the dynamic property may well differ. A second point of concern is that dividing the system into an interacting central region and non-interacting leads is actually quite subtle.

3.4. Model Hamiltonian

We split the total Hamiltonian in three pieces: $H = H_c + H_T + H_{cen}$. where, H_c describes the contacts, H_T is the tunneling coupling between contacts and the interacting region, and

H_{cen} , models the interacting central region, respectively. Below we discuss each of these terms.

3.4.1. Contact Hamiltonian

Guided by the typical experimental geometry in which the leads rapidly broaden in to metallic contacts, we view electrons in the leads as non interacting except for an overall self-consistent potential. Thus, the contact Hamiltonian is

$$H_c = \sum_{k\alpha \in L,R} \epsilon_{k\alpha} C_{k\alpha}^+ C_{k\alpha}, \quad (3.4.1)$$

in this summation and the Green functions in the leads for the uncoupled system are:

$$\begin{aligned} g_{k\alpha}^<(t-t') &= i \langle C_{k\alpha}^+(t) C_{k\alpha}(t') \rangle \\ &= i f(\epsilon_{k\alpha}^0) \exp[-i\epsilon_{k\alpha}(t-t')], \end{aligned} \quad (3.4.2)$$

and

$$\begin{aligned} g_{k\alpha}^{r,a}(t-t') &= \mp i \theta(\pm t \mp t') \langle \{ C_{k\alpha}(t), C_{k\alpha}^+(t') \} \rangle \\ &= \mp i \theta(\pm t \mp t') \exp[-i\epsilon_{k\alpha}(t-t')]. \end{aligned} \quad (3.4.3)$$

Here, $f(\epsilon_{k\alpha}) = [\exp[(\epsilon_{k\alpha} - \mu_\alpha)/k_B T] + 1]^{-1}$ is the equilibrium distribution in a given lead. Here, $C_{k\alpha}$ denotes creation (distraction) of carriers in the single – particle state α , and θ is the amplitude of occupation of states

3.4.2. Tunneling Hamiltonian

The coupling constants between the leads and the central (interacting) region depend, in principle, on the actual charge densities (accumulation and depletion regions, charge build-up in the central region, etc.), and they should be determined via a self-consistent calculation. This program has been completed by combining the density functional theory (DFT) with the non-equilibrium Green function theory (see, e. g, [24]), and will be briefly addressed later. Here, however, we assume these parameters as known, and write

$$H_T = \sum_{k\alpha \in \epsilon} [v_{k\alpha,n} C_{k\alpha}^+ d_n + h.c.]. \quad (3.4.4)$$

Here, $\{d_n^+\}$ and $\{d_n\}$ are the single-electron creation and annihilation operators for the complete and orthonormal set of the states $|n\rangle$ in the interacting regions.

3.4.3. Central Region Hamiltonian

The form chosen for the central region Hamiltonian H_{cen} depends on geometry and on the physical behavior being investigated. We will discuss three particular examples in detail.

3.4.3.1. Central Region in Non-Interacting Levels

In the first, the central region is taken to consist of non-interacting levels,

$$H_{cen} = \sum_m \epsilon_m d_m^\dagger d_m. \quad (3.4.5)$$

Here, d_m^\dagger (d_m) creates (destroys) an electron in state m .

The choice (3.4.5) represents a simple model for resonant tunneling. Below we shall present general results for an arbitrary number of levels, and analyze the case of a single level, which is exactly solvable in detail.

3.4.3.2. Central Region Couple To Phonon

The second example we will discuss is a situation where the states in the central region couple to phonons:

$$H_{cen}^{el-ph} = \epsilon_0 d^\dagger d + \sum_q M_q [a_q^\dagger + a_{-q}] \quad (3.4.6)$$

Here, the first term represents a single electronic state, while the second term represents interaction of an electron in that level with phonons: a_q^\dagger (a_q) creates (destroys) a phonon in mode q , and M_q is the interaction matrix element. The full Hamiltonian of the system must also include the free phonon contribution

$H_{ph} = \sum_q \hbar \omega_q a_q^\dagger a_q$. This example, while not exactly solvable, is helpful to show how interactions influence the current.

3.4.3.3. Anderson-Type Model (Electron-Electron Interactions)

The final example consists of an Anderson-type model [23] for electron-electron interactions in the central region:

$$H_{cen} = \sum_\delta \epsilon_\delta d_\delta^\dagger d_\delta + u_{n\uparrow n\downarrow}. \quad (3.4.7)$$

Here, δ is a spin-level, n_δ is the occupation number operator of spin-state δ , and U describes the on-site Coulombic repulsion. This model has been the topic of intense study because of the very rich (complicated) physics that it describes. For example, in the low temperature limit it exhibits Kondo behavior.

In the high temperature limit the equation-of-motion technique allows a relatively simple analysis, which we will discuss in some detail.

3.5. General Expression for the Current

The current from the left contact through left barrier to the central region can be calculated from the time evolution of the occupation number operator of the left contact:

$$J_L = -e \langle \dot{N}_L \rangle = -\frac{ie}{\hbar} \langle [H, N_L] \rangle. \quad (3.5.1)$$

$$\text{where, } N_L = \sum_{k,\alpha \in L} c_{k\alpha}^\dagger c_{k\alpha} \quad \text{and } H = H_c + H_T + H_{cen}.$$

Since H_c and H_{cen} commute with N_L , one readily finds:

$$J_L = \frac{ie}{\hbar} \sum_{k,\alpha \in L} [V_{k\alpha,n} \langle c_{k\alpha}^\dagger \mathbf{d}_n \rangle - V_{k\alpha,n}^* \langle \mathbf{d}_n^\dagger c_{k\alpha} \rangle]. \quad (3.5.2)$$

Now define two new Green functions (we set $\hbar=1$, and reintroduce it in the final expression for the current):

$$\begin{aligned} G_{n,k\alpha}^<(t-t') &\equiv i \langle c_{k\alpha}^\dagger(t') d_n(t) \rangle \\ G_{k\alpha,n}^<(t-t') &\equiv i \langle d_n^\dagger(t') c_{k\alpha}(t) \rangle. \end{aligned} \quad (3.5.3)$$

We see that the current is given by the time-diagonal components of the Green function defined in (3.5.3). These functions have the property

$G_{k\alpha,n}^<(t,t) = - [G_{n,k\alpha}^<(t,t)]^*$ and inserting then time-labels, the current can be expressed as

$$J_L = \frac{2e}{\hbar} \text{Re} [\sum_{k,\alpha \in L} V_{k\alpha,n} G_{n,k\alpha}^<(t,t)]. \quad (3.5.4)$$

Next, one needs an expression for $G_{n,k\alpha}^<(t-t')$. For the present case, with non-interacting leads, a general relation for the contour-ordered Green function $G_{n,k\alpha}(\tau, \tau')$ can be derived

rather easily with the equation-of-motion technique. Since the non-equilibrium theory is structurally equivalent to equilibrium theory, it is sufficient to consider the $T=0$ equation-of-motion for the time-ordered Green function $G_{n,k\alpha}^+$:

$$-i \frac{\partial}{\partial t'} G_{n,k\alpha}^+(t-t') = \epsilon_{k\alpha} G_{n,k\alpha}^+(t-t') + \sum_m G_{nm}^+(t-t') V_{k\alpha,m}^* \quad (3.5.5)$$

Where we defined the central region time-ordered Green function $G_{nm}^+(t-t') = -i \langle T \{ d_n(t) d_m^\dagger(t') \} \rangle$. Note that it is crucial that the leads be non interaction; had we allowed interactions in the leads, the equation of motion technique would have generated higher order Green functions in (3.5.5), and we would not have a closed set of equations.

We can interpret the factor $(-\partial_{t'} - \epsilon_{k\alpha})$ multiplying $G_{n,k\alpha}^+(t-t')$ as the inverse of the contact Green function operator (working from right-hand side), and introduce a short-hand notation:

$G_{n,k\alpha}^t g_{k\alpha}^{-1} = \sum_m G_{nm}^t V_{k\alpha,m}^*$. By operating with $g_{k\alpha}^t$ from right, we arrive at

$$G_{n,k\alpha}^t(t-t') = \sum_m \int dt_1 G_{nm}^t(t-t_1) V_{k\alpha,m}^* g_{k\alpha}^t(t_1-t'). \quad (3.5.6)$$

According to analytic continuation rules, this equation has in non-equilibrium precisely the same form, except that the intermediate time integration runs on the complex contour:

$$G_{n,k\alpha}(\tau, \tau') = \sum_m \int d\tau_1 G_{nm}(\tau, \tau_1) V_{k\alpha,m}^* g_{k\alpha}(\tau_1, \tau'). \quad (3.5.7)$$

Here $G_{nm}(\tau, \tau_1)$ is the contour-ordered Green function for the central region.

3.6 Current Conservation

Any meaningful theory of current must respect current conservation. Here we examine what implications this necessary requirement has on the derived expressions for the current flowing between the contacts and the central region. The retarded Green function (G^r) differs from zero only for time $t \geq t'$. This function can be used to calculate the response at time t to an earlier perturbation of the system at time t' . The advanced Green function (G^a) is only finite for $t \leq t'$. The ‘‘lesser than’’ Green function is also called the particle propagator, while the ‘‘greater than’’ Green function, in which the order of the creation and annihilation operators are reversed, is called the hole propagator. This observation is the

precursor of a more fundamental difference between the lesser/greater and retarded/advanced functions; this difference will be accentuated under non-equilibrium conditions. These various functions are not independent: they obey

$$G^r - G^a = G^> - G^<.$$

Using this general relationship $G^r - G^a = G^> - G^<$, valid for both contact and central region Green functions,

$$\begin{aligned} J_L &= \frac{e}{\hbar} \int \frac{d\varepsilon}{2\pi} \sum_{k,\alpha\in n,m,L} V_{k\alpha,n} V_{k\alpha,m}^* [G_{nm}^>(\varepsilon) g_{k\alpha}^<(\varepsilon) - G_{nm}^<(\varepsilon) g_{k\alpha}^>(\varepsilon)] \\ &= \frac{e}{\hbar} \int \frac{d\varepsilon}{2\pi} \sum_{\alpha\in L,n,m} [G_{nm}^>(\varepsilon) \Sigma_{\alpha,mn}^<(\varepsilon) - G_{nm}^<(\varepsilon) \Sigma_{\alpha,mn}^>(\varepsilon)] \\ &= \frac{e}{\hbar} \int \frac{d\varepsilon}{2\pi} \text{Tr} \{ G^> \Sigma_L^< - G^< \Sigma_L^> \}, \end{aligned} \quad (3.6.1)$$

where we have defined the tunneling self-energy $\Sigma = \Sigma V^* g V$

$$\begin{aligned} \Sigma_{\alpha,mn}^{r,a}(\varepsilon) &= \sum_k V_{k\alpha,m}^* g_{k\alpha}^{r,a}(\varepsilon) V_{k\alpha,n} = \Lambda_{mn}^\alpha(\varepsilon) \mp \frac{i}{2} \Gamma_{mn}^\alpha(\varepsilon) \\ \Sigma_{\alpha,mn}^<(\varepsilon) &= \sum_k V_{k\alpha,m}^* g_{k\alpha}^<(\varepsilon) V_{k\alpha,n} = i \Gamma_{mn}^\alpha(\varepsilon) f_\alpha(\varepsilon) \\ \Sigma_{\alpha,mn}^>(\varepsilon) &= \sum_k V_{k\alpha,m}^* g_{k\alpha}^>(\varepsilon) V_{k\alpha,n} = -i \Gamma_{mn}^\alpha(\varepsilon) [1 - f_\alpha(\varepsilon)]. \end{aligned} \quad (3.6.2)$$

The current formula (3.6.1) has an obvious physical interpretation: the current flowing out of the left contact (first term) is proportional to $\Sigma_L^<$, which gives the out-tunneling rate of the occupied states in the left contact, and to $G^>$, which gives the number of available states in the central region. The second term, with opposite sign, gives then the current flowing from the central region to the left contact. We next define the total self-energy, which is the sum of tunneling contributions, and the interactions residing in the central region:

$$\Sigma_{\text{tot}} = \Sigma_{\text{int}} + \Sigma_L + \Sigma_R. \quad (3.6.3)$$

The condition for current conservation is $J_L + J_R = 0$, and we shall now show that this condition imposes a sum-rule for the interacting self-energy. To do this, we first note that the Keldysh equations for the lesser and greater Green functions, $G^{<>} = G^r \Sigma_{\text{tot}}^{<>} G^a$ can be combined to yield

$$(G^r)^{-1} - (G^a)^{-1} = \Sigma_{tot}^< - \Sigma_{tot}^>, \quad (3.6.4)$$

which allows us to do the following manipulation:

$$\begin{aligned} \text{Tr} \{ \Sigma_{tot}^< G^> - \Sigma_{tot}^> G^< \} &= \text{Tr} \{ \Sigma_{tot}^< G^r \Sigma_{tot}^> G^a - \Sigma_{tot}^> G^r \Sigma_{tot}^< G^a \} \\ &= \text{Tr} \Sigma_{tot}^< G^r [\Sigma_{tot}^< - (G^r)^{-1} + (G^a)^{-1}] G^a - [\Sigma_{tot}^< - (G^r)^{-1} + (G^a)^{-1}] G^r \Sigma_{tot}^< G^a = 0 \end{aligned} \quad (3.6.5)$$

where we repeatedly used the cyclic property of Trace. The condition for current conservation thus becomes

$$J_L + J_R = \frac{e}{\hbar} \int \frac{d\omega}{2\pi} \text{Tr} \{ (\Sigma_{tot}^< - \Sigma_{int}^<) G^> - (\Sigma_{tot}^> - \Sigma_{int}^>) G^< \} = 0 \quad (3.6.6)$$

which, using (3.6.5), implies a necessary condition that any model self-energy Σ_{int} must satisfy:

$$\int \frac{d\omega}{2\pi} \text{Tr} \{ \Sigma_{int}^< G^> - \Sigma_{int}^> G^< \} = 0. \quad (3.6.7)$$

The self – consistent Born approximation (both for impurity scattering or electron-phonon interaction) is an example of a conserving approximation.

3.7 Non Interacting Resonant-Level Model

In the non-interacting case (or mean – field models), the Hamiltonian is $H = H_C + H_T + H_{cen}$,

Where $H_{cen} = \sum_n \epsilon_n d_n^\dagger d_n$. The Dyson and Keldysh equations are now

$$\begin{aligned} G^r(\epsilon) &= g^r(\epsilon) + g^r(\epsilon) \Sigma^r(\epsilon) G^r(\epsilon) \\ G^<(\epsilon) &= G^r(\epsilon) \Sigma^<(\epsilon) G^a(\epsilon), \end{aligned} \quad (3.7.1)$$

Where the self-energy is given by (3.6.2) $\Sigma = \Sigma_L + \Sigma_R$. Upon substituting (3.7.1) in the expression for the tunneling current (3.6.1), one finds a very compact result:

$$J_L = \frac{e}{\hbar} \int \frac{d\epsilon}{2\pi} T(\epsilon) [f_L(\epsilon) - f_R(\epsilon)], \quad (3.7.2)$$

where the transmission probability $T(\epsilon)$ is given by

$$T(\epsilon) = \text{Tr} \{ \Gamma^L(\epsilon) G^r(\epsilon) \Gamma^R(\epsilon) G^a(\epsilon) \} \quad (3.7.3)$$

This equation has found many applications, but it should be recalled that it is valid only in the case when interactions can be modeled by one-body potentials, i.e., the interaction self-

energies must be one-point functions with vanishing lesser and greater components. In general, the solution of Eqs.(3.7.1) require matrix inversion. In the case of a single level, the scalar equations can be readily solved. Using the identity

$$G^r G^a = \frac{G^a}{G^{a-1} - G^{r-1}} = \frac{\Lambda(\varepsilon)}{\Gamma(\varepsilon)}, \quad (3.7.4)$$

where $A(\varepsilon) = i[G^r(\varepsilon) - G^a(\varepsilon)]$ is the spectral function, one can write $G^<$ in a “pseudo equilibrium” form :

$$G^<(\varepsilon) = i A(\varepsilon) \hat{f}(\varepsilon), \quad (3.7.5)$$

$$\text{where } \hat{f}(\varepsilon) = \frac{\Gamma^L(\varepsilon)f_{L(\varepsilon)} + \Gamma^R(\varepsilon)f_{R(\varepsilon)}}{\Gamma(\varepsilon)}, \quad (3.7.6)$$

$$A(\varepsilon) = \frac{\Gamma(\varepsilon)}{[\varepsilon - \varepsilon_0 - \Lambda(\varepsilon)]^2 + [\frac{\Gamma(\varepsilon)}{2}]^2}. \quad (3.7.7)$$

The current (3.6.1) becomes now

$$J = \frac{e}{\hbar} \int \frac{d\varepsilon}{2\pi} \frac{\Gamma^L(\varepsilon)\Gamma^R(\varepsilon)}{[\varepsilon - \varepsilon_0 - \Lambda(\varepsilon)]^2 + [\Gamma(\varepsilon)/2]^2} [f_L(\varepsilon) - f_R(\varepsilon)]. \quad (3.7.8)$$

Note that this derivation made no assumptions about proportionate coupling to the leads. The factor multiplying the difference of the Fermi function is the familiar expression for elastic transmission coefficient $T(\varepsilon)$ through a resonant level. It is important to understand the difference between this result and the result obtained in section 3.5. To further emphasis the difference, let us now suppose that the green function for the interaction central region can be solved: $G^{r,a}(\varepsilon) = [\varepsilon - \varepsilon_0 - \lambda(\varepsilon) \pm i\gamma(\varepsilon)/2]^{-1}$, where λ and $\gamma/2$ are the real and imaginary parts of the self-energy(including interactions and tunneling). Then the interacting result for coupling becomes

$$J = \frac{e}{\hbar} \int \frac{d\varepsilon}{2\pi} [f_L(\varepsilon) - f_R(\varepsilon)] \frac{\Gamma^L(\varepsilon)\Gamma^R(\varepsilon)}{\Gamma^L(\varepsilon) + \Gamma^R(\varepsilon)} \times \frac{\gamma(\varepsilon)}{[\varepsilon - \varepsilon_0 - \Lambda(\varepsilon)]^2 + [\gamma(\varepsilon)/2]^2} \quad (3.7.9)$$

This result coincides with the non-interacting current expression (3.7.8) if $\lambda(\varepsilon) \rightarrow \Lambda(\varepsilon)$ and $\gamma(\varepsilon) \rightarrow \Gamma(\varepsilon) = \Gamma^L(\varepsilon) + \Gamma^R(\varepsilon)$. In phenomenological model, where the total level-width is expressed as a sum of elastic and inelastic widths, $= \gamma_e + \gamma_i$, one recovers

the results of Jonson and Grincwajg [25], and Weil and Vinter [26]. If the level-width and level-shift functions Γ and Λ are energy independent, it is easy to get the current-voltage characteristics. The zero-temperature IV-characteristics then presented in (fig 3.1).

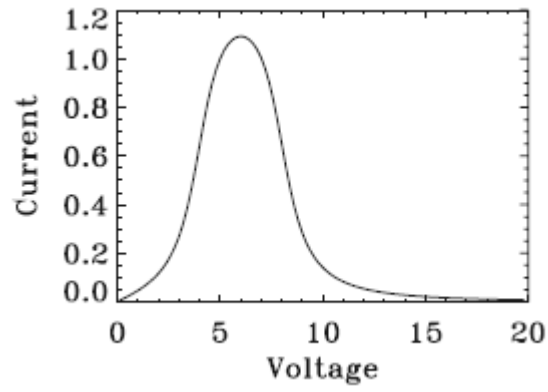


Fig 3.1 IV-characteristics for a model resonant tunneling device.

SUMMARY AND CONCLUSION

Semiconductor is a solid material with a conductivity of much more than insulator, but less than metal. One of the important insight of semiconductor material its energy gap (E_g). Semiconductor has large energy than metal and less than insulator materials. The band gap is the difference in energy between lowest point called the valance band and the highest band called the conduction band. The concentrations of electrons in conduction band and holes in the valance band are dependent on the temperature. At absolute temperature the valance band is full of carriers whereas conduction band is empty. However, when the temperature increased, electrons are excited from the valance band to the conduction band across the energy gap. These thermally excited electrons are capable of conducting, while the hole can occur in the band out of which they have been excited. In order to clarify the general behavior and electrical properties of semiconductor device, it's necessary to know the number of charges per volume in the material. The Fermi-Dirac distribution function is an important parameters used to determine the probability of an energy state that was occupied by the electrons at temperature T . So that, at the absolute zero-temperature, all the lowest energy level known as Fermi level.

Pure semiconductor with no impurities is called an intrinsic semiconductor and impure (doped) semiconductor material is called extrinsic semiconductor. The types of impurity levels in extrinsic semiconductor suited inside forbidden band are donor and acceptor levels. In n-type semiconductor there is a high concentration of electrons in the conduction band compared with the hole concentration in valance band. In p-type semiconductor, there is a high concentration of holes in the valance band as compared to the electron concentration in the conduction band. When one or more of the dimension of a solid are reduced sufficiently in size, its physic-chemical behavior departs significantly from that of bulk state. Within reduction in size, different and often new electrical, mechanical, chemical, magnetic and optical property emerges. The resulting structure is a low dimensional structure. The confinement of particles in a low-dimensional structure leads to a dramatic change in their behavior and to the manifestation of novel-size dependent effects which usually fall in to the category of quantum size effects [27]. In this end, classically treating transport behavior of particles in such novel device are non-physical

properties. Semiconductor with dimensions of 10nm and smaller are called semiconductor nanostructure structure.

Depending on the number of directions along which the electron motion is confined, semiconductor-nanostructures are: Quantum Wells (2D), quantum wire (1D) and quantum dots (0D). the unique physical and chemical properties of semiconductor nano material make it suitable for application emerging technologies, such as nano electronics, solar cells, non-linear optics, biomedicine etc. the motion of carries in a bulk material has been treated by classical transport theory mostly in Boltzmann distribution functions, however, the motions of carriers in nanostructure device has been treated with quantum transport theory. Besides to coherent transport phenomena characterizing the transient response of the system, review of theoretical description has allowed the study of scattering induced phase coherence in steady-state condition. Transport in mesoscopic phenomena is the phase coherence of the charge carriers which maintained over a significant part of the transport process. The interference effects resulting from this phase coherence are reflected in a number of experimentally measurable properties such as weak localization, Aharonov-Bohm effect, and universal conductance fluctuations. Many of these phenomena can be observed in a bulk samples.

It is natural to divide mesoscopic transport in to stationary and time-dependent phenomena. Stationary transport properties of tunneling structures such as double-barrier semiconductor heterostructures, super lattices, metallic nano wires, and coulomb blockade structures are treated as examples for quantum transport through mesoscopic systems. A central issue is the treatment of interactions in the mesoscopic region, and, as we shall see, non-equilibrium Green function techniques are well suited for this purpose. The modern reformulation of these ideas, due to Meir and Wingreen [28] has led to a veritable explosion in the number of papers addressing these issues, which use the Keldysh approach to interacting mesoscopic transport. A full account of all of this work is obviously impossible; instead we will concentrate on a few central results. A key issue is that under certain conditions, a Landauer-type conductance formula can be derived. The Landauer formula relates the conductance of a mesoscopic sample [which is connected via "ideal" leads to

two (or more) reservoirs] to its transmission properties. Conductance formula have played an important role in the analyses of many mesoscopic transport phenomena and it is therefore of interest to investigate whether interactions and /or time-dependence can be treated in a similar fashion in non-equilibrium Green function formalism.

CONCLUSIONS

Our important review conclusion is that the different levels may have different couplings to the leads, and it is reasonable to assume that the higher the energy of a given level is, the more strongly it couples to the leads. The conductance shows periodic peaks as a function of gate voltage (v_g) which moves the energy levels of the central region with respect to the lead energy levels, or, equivalently, moves the chemical potential of the leads. The periodicity of the conductance oscillations is explained quite readily with the charging energy U of the central region; however, more interesting is that the individual conductance peaks show complicated temperature dependence. Another important observation is that the conductance peaks remain resolved in temperatures much higher than the bare-energy-level spacing $\Delta\epsilon$, which is of the order of 0.05mev in the samples. This clearly shows that interaction effects are important (because in the non-interacting case all resonance features would be washed out if $k_B T > \Delta\epsilon$); one may estimate that the charging energy U is of the order of 0.5mev. Thus, in the temperature range $\Delta\epsilon < k_B T < U$ an anomalous temperature dependence can be expected.

Bibliography

1. R. Landauer, *IBM J. Res. and Dev.* 1,223 (1957)
2. S. Datt, *Electronic transport in mesoscopic systems* (Cambridge University Press, Cambridge,1995)
3. K.V. Klitzing, G. Dorda, and M. Pepper; *Phys. Rev. Lett.* 45, 494 (1980)
4. B. J. Van Wees; *Phys.Rev.Lett.* 60,848 (1988)
5. D.A. Wharam et al.; *J. Phys .C: Solid State Physics* 21, L209 (1988)
6. D. K. Ferry, S.M. Goodnick , and J. Bird, *Transport in Nanostructures, 2ed.*(Cambridge University Press,Cambridge,2009)
7. K.J. Thomas et al.; *Phys. Rev. Lett.* 77, 135 (1996)
8. O .Kalman, *Quantum Interference in semiconductor Ring, PhD thesis, University of Szeged,2009.*
9. D. Bercioux, *Spin-orbit interactions in semiconductor nanostructures, [http; // ftp1.physik.uni-freiburg.de /teaching/ Nano electronics /](http://ftp1.physik.uni-freiburg.de/teaching/Nano_electronics/).*
10. W.Walukiewicz, H.E. Ruda, J. Lagowski, and H.C. Gatos, *Phys. Rev.* B30,4571 (1984).
11. J .Solym, *A modern Szilard test fizikaalapai* (ELTE Eötvös Kiado ,Budapest, 2003)
12. Y. Murayama, *Mesoscopic Systems; Fundamentals and Applications* (Wiley-VCH, NewYork, 2001)
13. G.H.Wannier, *Phys.Rev.* 52, 191 (1937).
14. R. Peierls, *Z.Phys.* 80 (1933).
15. D.R.Hofstadter, *Phys.Rev.* B14, 2239 (1976).
16. K .Jimenez-Garcia etal.; *Phys.Rev.Lett.* 108,225303 (2012).

17. J. Kong et al.; *Phys.Rev.Lett.*87, 106801 (2001).
18. C.C. Eugster and J.A. del Alamo, *Phys.Rev.Lett.*67,3586 (1991).
19. C-Cohen-Tannoudji, B.Diu, and F.Laloë *Quantum Mechanics Vol.1, 2ed.* (Wiley, NewYork, 1977).
20. M. Abramowitz and I. Stegun, editors, *Handbook of mathematical functions* (Dover Publications, New York,1965).
21. V.S.A. Sequoia, G.E. Stillman, and C.M. Wolfe, *Thin Solid Films* 31 (1976).
22. N. Agrait, C.untiedt, G.Rubio-Bollinger, S.Vieira; *Phys.Rev.Lett.*88, 216803 (2002).
23. P.W.Anderson; *Phys.Rev.*124, 41 (1961).
24. M.Brandbyge, J.L.Mozos, P. Ordejon, J.Taylor, K. Stokbro; *Phys. Rev. B* 65,165401 (2002).
25. M. Jonson, A. Grincwajg; *Appl. Phys. Lett.* 51, 1729 (1987)
26. T. Weil, B. Vinter; *Appl. Phys. Lett.* 50, 1281 (1987)
27. C.Jacoboni and P.Lugli, *The Monte Carlo Method for Semiconductor Device Simulation* (Springer, Wien, 1989)
28. Y. Meir, N. S. Wingreen; *Phy. Rev. Lett.* 68, 2512 (1992)